Measurement of Deformability of Cell by Slits between Micro Cylindrical Pillars

Yusuke TAKAHASHI, Shigehiro HASHIMOTO, Haruka HINO, Hiromi SUGIMOTO

Biomedical Engineering, Department of Mechanical Engineering,
Kogakuin University, Tokyo, 163-8677, Japan
http://www.mech.kogakuin.ac.jp/labs/bio/

ABSTRACT

Deformation of a cell has been measured using slits between micro cylindrical pillars *in vitro*. Micro cylindrical pillars (0.02 mm diameter, 0.06 mm height) were fabricated on the glass plate using the photolithography technique. Variation was made on the gap between pillars: 0.025 mm, 0.020 mm, 0.015 mm, and 0.010 mm. The micro pillars were set in the flow path between parallel plates, of which dimension of the cross section has 1 mm width and 0.06 mm height. Two types of biological cells were used in the test alternatively: C2C12 (mouse myoblast cell line), Hepa1-6 (mouse hepatoma cell line). The suspension of cells was introduced into the slits, and the deformation of the cell at the slit was observed by the microscope. The experimental results show that several cells clogged in the slit of 0.01 mm, and the passing time of C2C12 is shorter than that of Hepa1-6 at the smaller deformation ratio. The designed slit has capability for evaluation of deformability of a cell.

Keywords: Biomedical Engineering, Deformability, C2C12, Hepa1-6, Photolithography and Micro Flow Channel.

1. INTRODUCTION

Biological cells can pass through narrow gaps: micro capillaries, or micro slits. The biological system sorts cells according to the size, deformability, and adsorptivity of the cell. Cells are sorted according to deformability through the gap or adsorptivity on the membrane *in vivo*. The mechanism might be applied to handle cells in diagnostics *in vitro*.

The deformability of cell was measured by several preparations *in viro*: through micro capillaries, and between counter rotating disks in the previous studies [1, 2]. The biological cell has the visco-elastic property.

The photolithography technique enables manufacturing a micro-channel. Several micro-fabrication processes have been designed to simulate the morphology of the microcirculation. In the previous studies, the micro slits were designed between micro cylindrical pillars [3, 4], or between micro ridges [5]. The micro-fabrication technique has also been applied to design microfluidic systems *in vitro* [6-12].

In the present study, deformation of a cell has been measured by slits between micro cylindrical pillars *in vitro*.

2. METHODS

Micro Slits
The micro slits have been designed between micro cylindrical pillars. The dimension of each micro cylindrical pillar is as follows: 0.025 mm diameter, and 0.06 mm height (Fig. 1)

Cylindrical pillars are arranged along the four lines by the photolithography technique. Each line is perpendicular to the flow direction of the channel. The pitch of lines is 0.5 mm. Each line has its own uniform gaps (*w*: the width of slits) between pillars. The gaps are 0.025 mm at the first line. The gap is 0.020 mm at the second line. The gaps are 0.015 mm at the third line. The gaps are 0.010 mm at the fourth line.

The micro slits are located at the middle part of the flow path between parallel plates, of which dimension of the cross section has 1 mm width (*W*), 30 mm length and 0.06 mm height (*H*) (Fig. 1). The flow path is constructed between parallel plates: the upper plate of polydimethylsiloxane (PDMS), and the lower plate of glass (S1111, Matsunami Glass Ind., Ltd., Japan). The upper plate has two holes of 5 mm diameter for the inlet and for the outlet of the flow of the cell suspension.

Photomask
The slide glass (S1111) plate (38 mm length, 26 mm width, and 1.0 mm thickness) was used for the base of the photomask (Fig. 2). The disk was dipped in the pure water and cleaned by the ultrasonic washer for five minutes.

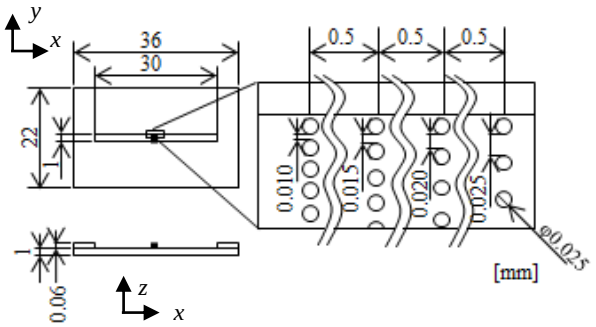

Fig. 1: Micro pillars in flow channel.

Before the vapor deposition of titanium, the surface of the glass plate was hydrophilized by the oxygen (30 cm^3/min, 0.1 Pa) plasma ashing for one minute at 100 W by the reactive ion etching system (FA-1, Samco Inc., Kyoto, Japan). Titanium was deposited on the surface of the glass plate with 100 nm thickness in the electron beam vapor deposition apparatus (3.1×10^{-4} Pa, 0.5 nm/s, 200 s, JBS-Z0501EVC JEOL Ltd., Tokyo, Japan). The oxygen (0.1 Pa, 30 cm^3/min) ashing was applied on the surface of the titanium in the reactive ion etching system (100 W, for one minute, FA-1).

To improve affinity between glass and photoresist material, HMDS (hexamethyldisilazane: Tokyo Chemical Industry Co., Ltd., Tokyo) was coated on the glass plate at 3000 rpm for 30 s with a spin coater. The positive photoresist material of OFPR-800LB (Tokyo Ohka Kogyo Co., Ltd, Tokyo, Japan) was coated on it with the spin coater (at 5000 rpm for 30 s). The photoresist was baked in the oven (DX401, Yamato Scientific Co., Ltd) at 368 K for three minutes.

The pattern for the slit was drawn on the mask with a laser drawing system (DDB-201K-KH, Neoark Corporation, Hachioji, Japan). To control the dimension of the pattern on the mold with the laser drawing system, the parameters were selected as follows: the voltage of 2.3 V, the velocity of 0.08 mm/s, the acceleration of 0.5 mm/s^2, and the focus offset at +0.4. The photoresist was baked in the oven (DX401, Yamato Scientific Co., Ltd) at 368 K for three minutes. The photoresist was baked in the oven (DX401) at 393 K for five minutes.

The photoresist was developed with tetra-methyl-ammonium hydroxide (NMD-3, Tokyo Ohka Kogyo Co., Ltd., Kawasaki, Japan) for one minute, rinsed with the distilled water, and dried by the spin-dryer (1100 rpm, 30 s, with N_2 gas, SF-250, Japan Create Co., Ltd., Tokorozawa, Japan). After confirmation of free of residual resists by the microscope, the titanium coated plate was etched with the plasma gas using RIE-10NR (Samco International, Kyoto, Japan). For etching, the gas of SF_6 (50 cm^3/min at 1013 hPa) with Ar (50 cm^3/min at 1013 hPa) was applied at 100 W at 4 Pa for five minutes. The residual OFPR-800LB was removed by acetone. The plate was dipped in the distilled water in one minute, after it is dipped in ethanol for one minute. The plate was dried by the spin-dryer: 300 rpm for 30 s with the distilled water, and 1100 rpm for 30 s with N_2 gas).

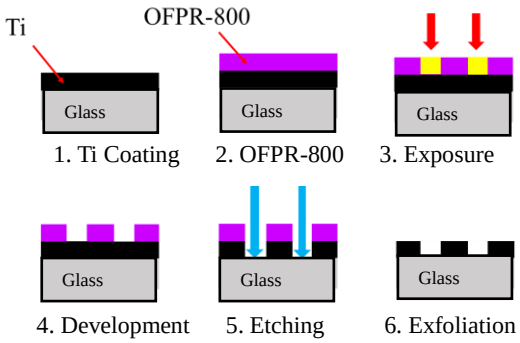

Fig. 2: Process for fabrication of photomask.

Micro Cylindrical Pillars on Lower Plate

The slide glass (26 mm × 38 mm × 1 mm) was used for the base of micro cylindrical pillars, after cleaning with acetone (Fig. 3). The surface of the glass plate was hydrophilized by the oxygen (30 cm^3/min, 0.1 Pa) plasma ashing for five minutes at 100 W by the reactive ion etching system (FA-1). The negative photoresist material of high viscosity (SU8-100: Micro Chem Corp., MA, USA) was coated on the slide glass at 3000 rpm for 30 s with a spin coater. The photoresist was baked at the hotplate at 338 K for three hours. The photoresist was exposed to the UV light through the mask in the mask aligner (M-1S, Mikasa Co. Ltd., Japan) at 15 mW/cm^2 for 14 s. The photoresist was baked at the hotplate in two processes: at 338 K for one minute, and at 368 K for ten minutes. The photoresist was developed with SU-8 Developer (Micro Chem Corp., USA) for ten minutes. The glass surface with the micro pattern was rinsed with IPA (2-propanol, Wako Pure Chemical Industries, Ltd.) for one minute, and pure water for one minute. The pattern was baked at the hotplate at 393 K for five minutes.

At the end of the process, the micro morphology of the surface with the micro pillars was observed by a scanning electron microscope (JSM6360, JEOL Ltd., Japan) (Fig. 7).

Upper Plate

After the slide glass plate was enclosed with a peripheral wall of polyimide tape, PDMS (Sylgard 184 Silicone Elastomer Base, Dow Corning Corp., MI, USA) was poured with the curing agent (Sylgard 184 Silicone Elastomer Curing Agent, Dow Corning Corp., MI, USA) on the mold (Fig. 5D). The volume ratio of PDMS to curing agent is ten to one. After degassing, PDMS was baked at 333 K for one hour in an oven (DX401, Yamato Scientific Co., Ltd). The baked plate of PDMS (3 mm thickness) was exfoliated from the slide glass plate. The PDMS plate was cut to make a rectangular upper plate for the flow channel. Two holes with the interval of 25 mm were punched by a punching tool (trepan MK405, Kai Industries Co., Ltd., Gifu, Japan) to make the inlet and the outlet. The upper plate was stuck on the lower plate with micro pattern adjusting the position of holes to make the flow channel. A rectangular parallelepiped channel is formed between upper and lower plates (Fig. 4). The two plates stick together with their surface affinity.

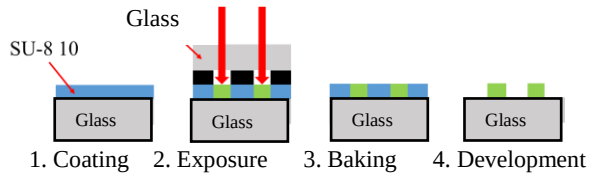

Fig. 3: Process for fabrication of pillars.

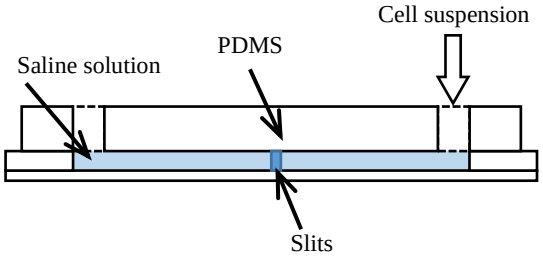

Fig. 4: Flow channel.

The flow channel is placed on the stage of the inverted phase contrast microscope (IX71, Olympus Co., Ltd., Tokyo).

Flow Test

Two kinds of biological cells were used in the test alternatively: C2C12 (mouse myoblast cell line originated with cross-striated muscle of C3H mouse), or Hepa1-6 (mouse hepatoma cell line of C57L mouse). Cells before the passage tenth were used in the flow test.

Cells (C2C12 and Hepa1-6) were cultured with the D-MEM (Dulbecco's Modified Eagle's Medium) containing 10% FBS and 1% of Antibiotic-Antimycotic (penicillin, streptomycin and amphotericin B, Life Technologies Japan Ltd., Tokyo, Japan) in the incubator. The medium was changed every two days.

Before the cells were proliferated to sub-confluent state, the cells were exfoliated from the plate of the culture dish with trypsin, and suspended in the medium. The cell suspension was diluted by the saline solution to be the suspension of the concentration of 10000 cells/cm^3 for the flow test.

Before the cell flow test, the surface of the flow channel was hydrophilized by the oxygen (30 cm^3/min, 0.1 Pa) plasma ashing for one minute at 100 W by the reactive ion etching system (FA-1). The channel was filled with the 4 % bovine albumin aqueous solution, and placed in the incubator for one hour to coat stable proteins on the inner surface of the channel.

The channel was washed out with the saline solution, and filled with the saline solution of 60 mm^3. The flow path was carefully examined to avoid mixing of air bubbles, which might stir the medium in the flow channel.

The 60 mm^3 of suspension of cells was added into the inlet port of the flow channel. The suspension of cells was introduced to the slits at the first line (w = 0.025 mm) by the pressure difference between the inlet and the outlet, which was kept by the gravitational level of the medium.

The capacity of the flow channel is 1.8 mm^3 (30 mm × 1 mm × 0.06 mm). The additional volume of 60 mm^3 makes the fluid level difference of 3 mm between inlet and outlet. The decrease ratio of the level difference between inlet and outlet is smaller than 10 % in ten seconds. The difference of 3 mm of the fluid (10^3 kg/m^3 density) produces the pressure difference of 0.03 kPa.

The cell passing through the slit was observed by the microscope, and recorded by the video camera (DSC-RX100M4, Sony Corporation, Japan), which is set at the eyepiece. Both the movement and the shape of the cell were analyzed by "ImageJ".

From the microscopic video image, the deformation ratio (R) of each cell in the slit was calculated by the following equation (Fig. 5).

$$R = d / w \qquad (1)$$

In Eq. 1, d is the diameter of the cell before deformation in the slit, and w is the width of the slit. R is unity, when the diameter of the cell equals to the width of the slit.

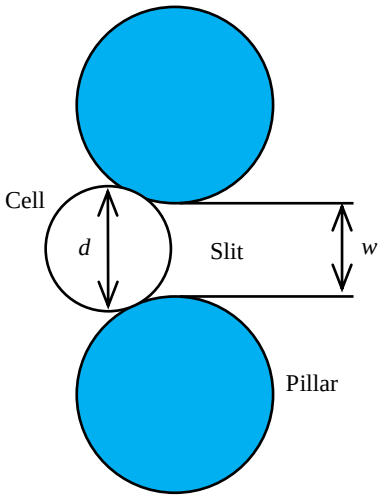

Fig. 5: Cell caught by slit between pillars.

The passing time (t) of each cell through the slit was measured. The relation between the passing time (t) and the deformation ratio (R) was plotted in Fig. 9. The relation approximated to the following linear equation.

$$t = a R + b \qquad (2)$$

3. RESULTS

Fig. 6 shows the floating cell of Hepa1-6. The diameters of cells suspended in the saline solution scatter around 0.02 mm. Fig. 7 shows the scanning electron microscope image of the micro pillars. Although several neighboring top surfaces of the micro cylindrical pillars make connections over the slit of 0.01 mm, the morphology of the gap between pillars keeps rectangular slit. The micro pillars stand perpendicular to the surface of the glass slide.

Fig. 8 exemplifies C2C12 passing through the slit (w = 0.01 mm) between micro pillars. The cell approaches to the slit between micro pillars (a), is captured between micro pillars (b), deforms to pass through the slit (c), and gets out from the slit (d). Several cells are clogged in the slits of 0.01 mm. Most of cells, on the other hand, pass through the slits wider than 0.015 mm.

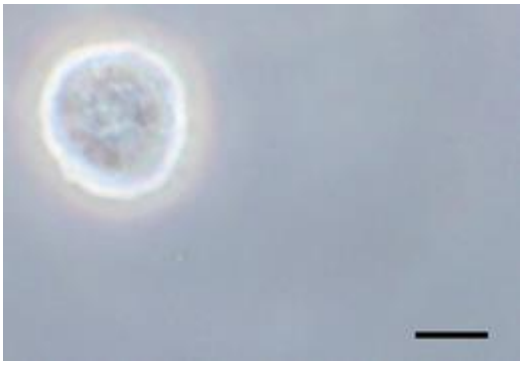

Fig. 6: Hepa1-6 suspended in saline solution: bar shows 0.01 mm.

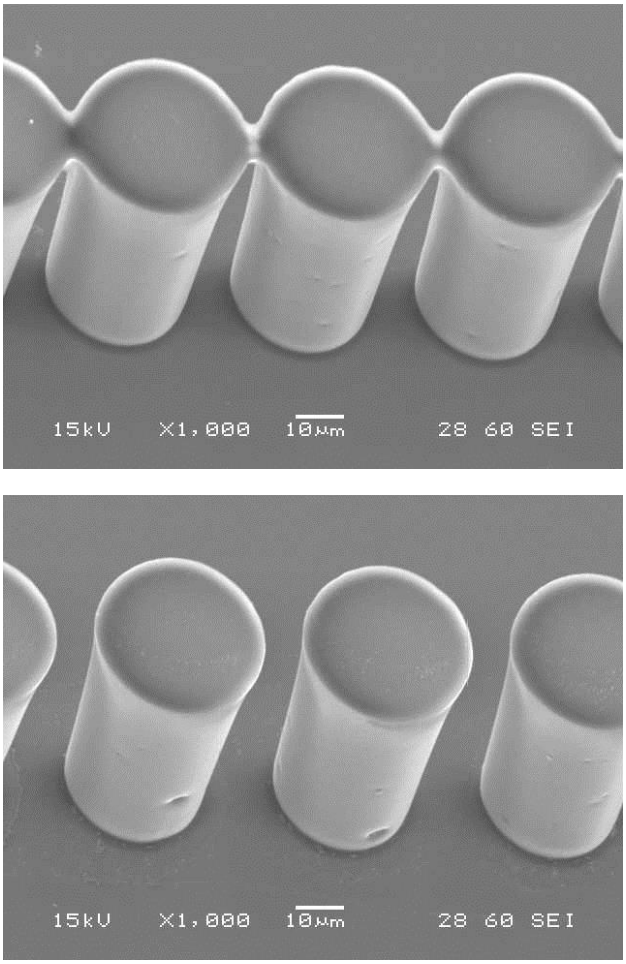

Fig. 7: Scanning electron microscope image of slit between micro pillars: w = 0.010 mm (upper), and w = 0.015 mm (lower).

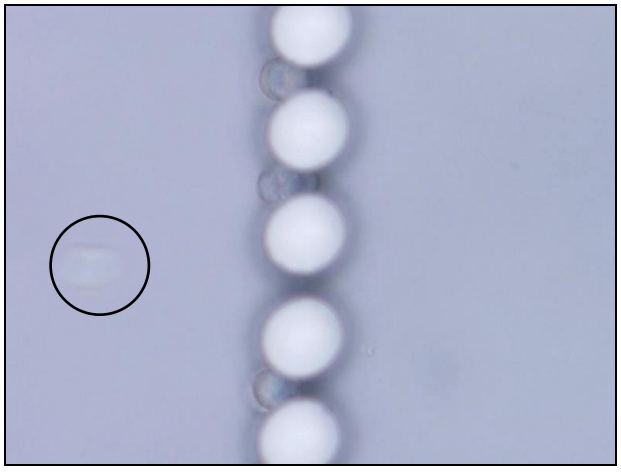

Fig. 8a: C2C12 (circled) approaches to micro cylindrical pillars (w = 0.01 mm): diameter of cylinder is 0.025 mm: flow from left to right.

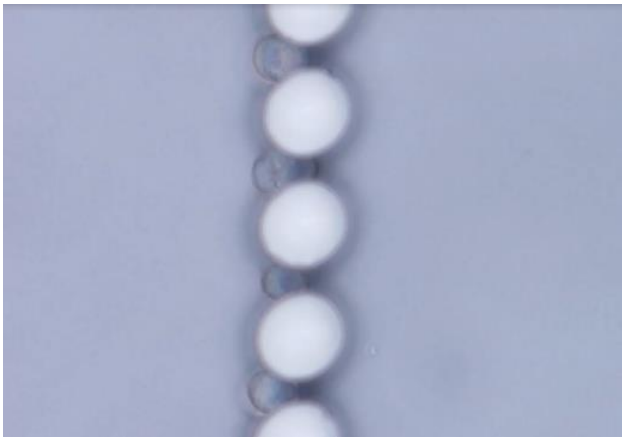

Fig. 8b: C2C12 is captured between micro cylindrical pillars (w = 0.01 mm): diameter of cylinder is 0.025 mm: flow from left to right.

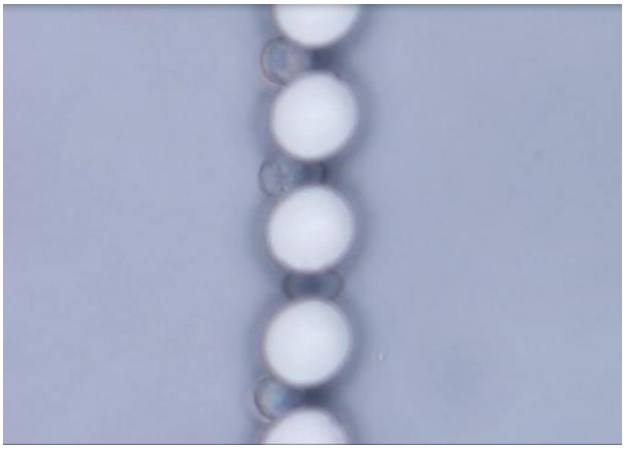

Fig. 8c: Deformed C2C12 goes through slit between micro cylindrical pillars (w = 0.01 mm): diameter of cylinder is 0.025 mm: flow from left to right.

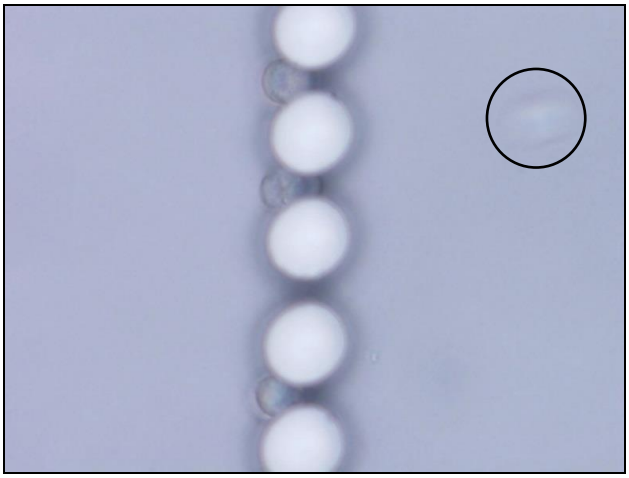

Fig. 8d: C2C12 (circled) gets out from slit between micro cylindrical pillars (w = 0.01 mm): diameter of cylinder is 0.025 mm: flow from left to right.

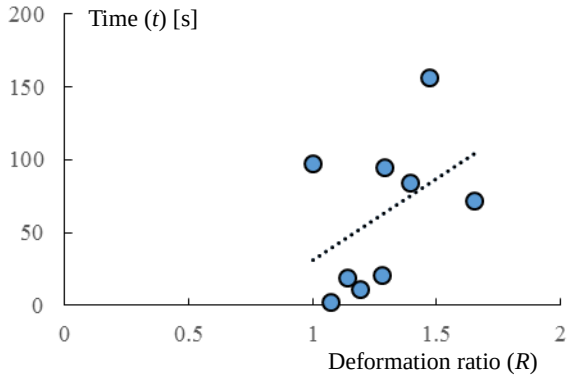

Fig. 9a: Time (t) [s] vs. deformation ratio (R): Hepa1-6: $t = 1.1\times10^2 R - 8.1\times10$.

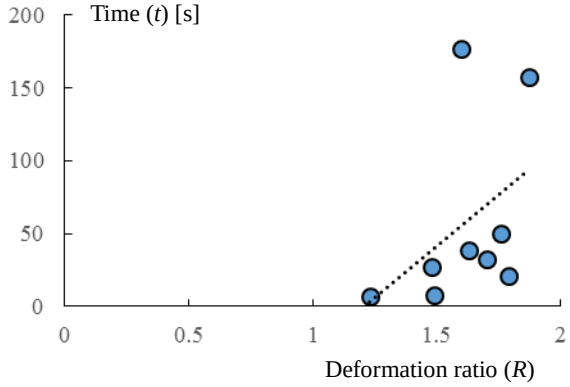

Fig. 9b: Time (t) [s] vs. deformation ratio (R): C2C12: $t = 1.4\times10^2 R - 1.7\times10^2$.

Fig. 9 shows the relation between the passing time (t) and the deformation ratio (R). In the range of R smaller than 1.5, the passing time (t) of C2C12 (Fig. 9b) is shorter than that of Hepa1-6 (Fig. 9a). In the range of R bigger than 1.5, data of the passing time scatters wider at C2C12 than at Hepa1-6. The coefficient (a) in Eq. 2 is higher at C2C12 (1.4×10^2 s) than Hepa1-6 (1.1×10^2 s). Among the passed cells, the maximum deformation ratios are 1.7 at Hepa1-6 and 1.9 at C2C12.

4. DISCUSSION

Preparation of the slit of sub micrometer is not easy. In the previous study, the slit of micrometer between pillars was manufactured by photolithography technique [4]. In another study, the micro slit was manufactured between ridges [5].

The slit in biological tissue has very short length (0.001 mm) and very narrow width (0.001 mm) with sub millimeter height *in vivo*. With the conventional machining technique, however, the slit with such kind of dimensions is not able to be made for *in vitro* test. The slit is fabricated between micro cylindrical pillars by photolithography technique in the present study.

Only one projection can be traced in the present experimental system. The cell can deform in the perpendicular direction. To observe the deformation in the perpendicular plane, the slit between upper and lower ridges is effective [5].

It is not easy to fabricate micro slit, keeping the rectangular shape smaller than 0.01 mm. The resistance of the flow channel is very high in the present experimental system. The resistance increases, when the cells clogged the slits in the flow channel. Internal pressure of the flow channel should be carefully controlled under the constant flow rate, otherwise the leakage or cavitation would occur. The flow path was carefully examined to avoid mixing of air bubbles, which might stir the medium in the flow channel. The small pressure difference between the inlet and the outlet of the flow channel is maintained around 0.03 kPa by the difference of the level of the fluid between the inlet and the outlet in the present study.

Several parameters have been applied to evaluate the deformability of biological cells: the maximum deformation ratio, and shear stress responsiveness [2]. The higher a shows that C2C12 takes longer time to be deformed to the higher ratio in the present study. The shorter passing time of C2C12 at the smaller deformation ratio shows that the frictional resistance might be smaller at C2C12 than Hepa1-6.

The capture of the cell at the slit depends on several factors: the dimension of the cell and the slit, deformation of the cell, the wall sear stress (shear rate) at the slit, and the affinity (charge) of the cell to the wall of the slit. The channel was filled with the 4 % bovine albumen aqueous solution, and placed in the incubator for one hour to coat stable proteins on the inner surface of the channel in the present study.

The adhesion of the cell in the flow depends on the morphology of the wall and the wall shear stress. The morphology of the defect on the wall of flow path might govern the capture of cells. The capture might depend on the property of the cell. The mechanism of adhesion might be applied to sort cells [13].

The experimental results might contribute to analyze adhesive mechanism of cancer cell during metastasis. The micro trap might simulate adhesive mechanism of flowing cells.

A red blood cell has flexibility and deforms in the shear flow [2]. It also passes through micro-circulation, of which the dimension is smaller than the diameter of the red blood cell. After circulation through the blood vessels for days, the red blood cell is trapped in the micro-circulation systems. Some cells can pass through the slit narrower than the capillary.

There are several methods to sort cells [13-22]. Non-invasive way is preferable to sort cells with minimum damage. Flow cytometry is one of the technologies, which is used for cell sorting. Cells suspended in the fluid are analyzed by the laser. The fluorescently labelled components in the cell are analyzed by the light emission.

5. CONCLUSION

Deformation of a cell has been measured using slits between micro cylindrical pillars *in vitro*. Slits of the width ($0.01 \text{ mm} < w < 0.025 \text{ mm}$) were fabricated between micro cylindrical pillars on the glass plate using the photolithography technique. The deformation of C2C12 (mouse myoblast cell line) and Hepa1-6 (mouse hepatoma cell line) at the slit was observed by the microscope. The experimental results show that several cells clogged in the slit of 0.01 mm, and the passing time of C2C12 is shorter than that of Hepa1-6 at the smaller

deformation ratio. The designed slit has capability for evaluation of deformability of a cell.

6. ACKNOWLEDGMENT

This work was supported by a Grant-in-Aid for Strategic Research Foundation at Private Universities from the Japanese Ministry of Education, Culture, Sports and Technology.

REFERENCES

[1] S. Hashimoto, "Detect of Sublethal Damage with Cyclic Deformation of Erythrocyte in Shear Flow", **Journal of Systemics Cybernetics and Informatics,** Vol. 12, No. 3, 2014, pp. 41-46.

[2] S. Hashimoto, et al., "Effect of Aging on Deformability of Erythrocytes in Shear Flow", **Journal of Systemics Cybernetics and Informatics**, Vol. 3, No. 1, 2005, pp. 90-93.

[3] Y. Takahashi, S. Hashimoto, H. Hino and T. Azuma, "Design of Slit between Micro Cylindrical Pillars for Cell Sorting", **Journal of Systemics, Cybernetics and Informatics**, Vol. 14, No. 6, 2016, pp. 8-14.

[4] S. Hashimoto, T. Horie, F. Sato, T. Yasuda and H. Fujie, "Behavior of Cells through Micro Slit", **Proc. 17th World Multi-Conference on Systemics Cybernetics and Informatics**, Vol. 1, 2013, pp. 7-12.

[5] A. Mizoi, Y. Takahashi, H. Hino, S. Hashimoto and T. Yasuda, "Deformation of Cell Passing through Micro Slit between Micro Ridges", **Proc. 20th World Multi-Conference on Systemics Cybernetics and Informatics**, Vol. 2, 2016, pp. 129-134.

[6] Y. Takahashi, S. Hashimoto, H. Hino, A. Mizoi and N. Noguchi, "Micro Groove for Trapping of Flowing Cell", **Journal of Systemics, Cybernetics and Informatics**, Vol. 13, No. 3, 2015, pp. 1-8.

[7] S.M. McFaul, B.K. Lin and H. Ma, "Cell Separation Based on Size and Deformability Using Microfluidic Funnel Ratchets", **Lab on a Chip - Miniaturisation for Chemistry and Biology**, Vol. 12, No. 13, 2012, pp. 2369-2376.

[8] E.D. Pratt, C. Huang, B.G. Hawkins, J.P. Gleghorn and B.J. Kirby, "Rare Cell Capture in Microfluidic Devices", **Chemical Engineering Science**, Vol. 66, No. 7, 2011, pp. 1508-1522.

[9] B. Yao, G.A. Luo, X. Feng, W. Wang, L.X. Chen and Y.M. Wang, "A Microfluidic Device Based on Gravity and Electric Force Driving for Flow Cytometry and Fluorescence Activated Cell Sorting", **Lab on a Chip - Miniaturisation for Chemistry and Biology**, Vol. 4, No. 6, 2004, pp. 603-607.

[10] D.R. Gossett, W.M. Weaver, A.J. Mach, S.C. Hur, H.T. Tse, W. Lee, H. Amini and D. DiCarlo, "Label-free Cell Separation and Sorting in Microfluidic Systems", **Analytical and Bioanalytical Chemistry**, Vol. 397, No. 8, 2010, pp. 3249-3267.

[11] A. Khademhosseini, J. Yeh, S. Jon, G. Eng, K.Y. Suh, J.A. Burdick and R. Langer, "Molded Polyethylene Glycol Microstructures for Capturing Cells within Microfluidic Channels", **Lab on a Chip**, Vol. 4, No. 5, 2004, pp. 425-430.

[12] J.C. Baret, O.J. Miller, V. Taly, M. Ryckelynck, A. El-Harrak, L. Frenz, C. Rick, M.L. Samuels, J.B. Hutchison, J.J. Agresti, D.R. Link, D.A. Weitz and A.D. Griffiths, "Fluorescence -activated Droplet Sorting (FADS): Efficient Microfluidic Cell Sorting Based on Enzymatic Activity", **Lab on a Chip**, Vol. 9, No. 13, 2009, pp. 1850-1858.

[13] M.R. King, L.T. Western, K. Rana and J.L. Liesveld, "Biomolecular Surfaces for the Capture and Reprogramming of Circulating Tumor Cells", **Journal of Bionic Engineering**, 2009, Vol. 6, No. 4, pp. 311-317.

[14] S.K. Lee, G.S. Kim, Y. Wu, D.J. Kim, Y. Lu, M. Kwak, L. Han, J.H. Hyung, J.K. Seol, C. Sander, A. Gonzalez, J. Li and R. Fan, "Nanowire Substrate-based Laser Scanning Cytometry for Quantitation of Circulating Tumor Cells", **Nano Letters**, Vol. 12, No. 6, 2012, pp. 2697-2704.

[15] H.M. Ji, V. Samper, Y. Chen, C.K. Heng, T.M. Lim and L. Yobas, "Silicon-based Microfilters for Whole Blood Cell Separation", **Biomedical Microdevices**, Vol. 10, 2008, pp. 251-257.

[16] M.S. Kim, T.S. Sim, Y.J. Kim, S.S. Kim, H. Jeong, J.M. Park, H.S. Moon, S.I. Kim, O. Gurel, S.S. Lee, J.G. Lee and J.C. Park, "SSA-MOA: A Novel CTC Isolation Platform Using Selective Size Amplification (SSA) and a Multi-obstacle Architecture (MOA) Filter", **Lab on a Chip - Miniaturisation for Chemistry and Biology**. Vol. 12, No. 16, 2012, pp. 2874-2880.

[17] A.Y. Fu, C. Spence, A. Scherer, F.H. Arnold and S.R. Quake, "A Microfabricated Fluorescence-Activated Cell Sorter", **Nature Biotechnology**, Vol. 17, 1999, pp. 1109-1111.

[18] S. Choi, J.M. Karp and R. Karnik, "Cell Sorting by Deterministic Cell Rolling", **Lab on a Chip - Miniaturisation for Chemistry and Biology**, Vol. 12, No. 8, 2012, pp. 1427-1430.

[19] H.N. Joensson, M. Uhlén and H.A. Svahn, "Droplet Size Based Separation by Deterministic Lateral Displacement-separating Droplets by Cell-induced Shrinking", **Lab on a Chip - Miniaturisation for Chemistry and Biology**, Vol. 11, No. 7, 2011, pp. 1305-1310.

[20] M. Cristofanilli, G.T. Budd, M.J. Ellis, A. Stopeck, J. Matera, M.C. Miller, J.M. Reuben, G.V. Doyle, W.J. Allard, L.W.M.M. Terstappen and D.F. Hayes, "Circulating Tumor Cells, Disease Progression, and Survival in Metastatic Breast Cancer", **New England Journal of Medicine**, Vol. 351, No. 8, 2004, pp. 781-791.

[21] H. Mohamed, L.D. McCurdy, D.H. Szarowski, S. Duva, J.N. Turner and M. Caggana, "Development of a Rare Cell Fractionation Device: Application for Cancer Detection", **IEEE Transactions on Nanobioscience**, Vol. 3, No. 4, 2004, pp. 251-256.

[22] S. Nagrath, L.V. Sequist, S. Maheswaran, D.W. Bell, D. Irimia, L. Ulkus, M.R. Smith, E.L. Kwak, S. Digumarthy, A. Muzikansky, P. Ryan, U.J. Balis, R.G. Tompkins, D.A. Haber and M. Toner, "Isolation of Rare Circulating Tumour Cells in Cancer Patients by Microchip Technology", **Nature**, Vol. 450, No. 7173, 2007, pp. 1235-1239.